European Journal of Pharmacology 634 (2010) 10–15

Contents lists available at ScienceDirect

European Journal of Pharmacology

journal homepage: www.elsevier.com/locate/ejphar

Molecular and Cellular Pharmacology

The effects of anandamide transport inhibitor AM404 on voltage-dependent calcium channels

Alp Alptekin [a], Sehammuddin Galadari [b], Yaroslav Shuba [c], Georg Petroianu [d], Murat Oz [d,e,*]

[a] Department of Anesthesiology, Yildirim Beyazit Training and Research Hospital, Ankara, 06270, Turkey
[b] Department of Biochemistry, Faculty of Medicine and Health Sciences, UAE University, Al Ain, United Arab Emirates
[c] Bogomoletz Institute of Physiology and International Center of Molecular Physiology, National Academy of Sciences of Ukraine, Kyiv-24, Ukraine
[d] Department of Pharmacology, Faculty of Medicine and Health Sciences, UAE University, Al Ain, United Arab Emirates
[e] National Institute on Drug Abuse, Integrative Neuroscience Section, 333 Cassell Drive, Baltimore MD, 21224, USA

ARTICLE INFO

Article history:
Received 21 September 2009
Received in revised form 30 January 2010
Accepted 9 February 2010
Available online 17 February 2010

Keywords:
Calcium channel
AM404
Endocannabinoid
Skeletal muscle

ABSTRACT

The effects of anandamide transport inhibitor AM404 were investigated on depolarization-induced $^{45}Ca^{2+}$ fluxes in transverse tubule membrane vesicles from rabbit skeletal muscle and on Ba2+ currents through L-type voltage-dependent Ca^{2+} channels in rat myotubes. AM404, at the concentration of 3 μM and higher, caused a significant inhibition of $^{45}Ca^{2+}$ fluxes. Radioligand binding studies indicated that the specific binding of [^{3}H] Isradipine to transverse tubule membranes was also inhibited significantly by AM404. In controls and in presence of 10 μM AM404, B_{max} values were 51 ± 6 and 27 ± 5 pM/mg, and *K*D values were 236 ± 43 and 220 ± 37 pM, respectively. Inhibitory effects of AEA and arachidonic acid on $^{45}Ca^{2+}$ flux and [^{3}H]Isradipine binding reported in earlier studies, were also enhanced significantly in the presence of AM404. In the presence of VDM11 (1 μM), another anandamide transport inhibitor, AM404 continued to inhibit $^{45}Ca^{2+}$ fluxes and [^{3}H]Isradipine binding. In rat myotubes, Ca^{2+} currents through L-type Ca^{2+} channels recorded in whole-cell configuration of patch clamp technique were inhibited by AM404 in a concentration-dependent manner with an IC_{50} value of 3.2 μM. In conclusion, results indicate that AM404 inhibits directly the function of L-type voltage-dependent Ca^{2+} channels in mammalian skeletal muscles.

Published by Elsevier B.V.

1. Introduction

Arachidonylethanolamide (anandamide, AEA) is an endogenously produced fatty acid ethanolamide that binds to cannabinoid (CB) receptors and produces cellular and pharmacological effects similar to Δ^9-THC, the psychoactive component of marijuana (for a review Howlett et al., 2002). Termination of AEA activity is achieved by the re-uptake of AEA via the putative anandamide membrane transporter and the hydrolysis of AEA by the fatty acid amide hydrolase, FAAH (for reviews; Di Marzo, 2008; Fowler, 2008). In earlier studies, several fatty acid-based molecules such as AM404 and VDM11 have been suggested to inhibit transport of AEA through cell membranes and widely employed in cellular and behavioral investigations of the endocannabinoid system (Di Marzo, 2008; Fowler, 2008).

We have previously shown that fatty acid based molecules including AEA (Oz et al., 2000), 2-Arachidonoylglycerol (Oz et al., 2004), and various unsaturated fatty acids (Oz et al., 2004; 2005) inhibit depolarization-induced $^{45}Ca^{2+}$ effluxes mediated by L-type voltage-dependent calcium channels (VDCCs), and the specific binding of [^{3}H]Isradipine to T-tubule membranes of rabbit skeletal muscles. In this study we hypothesized that AEA transport blocker AM404, based on its structural similarity to AEA and arachidonic acid can also modulate the function of L-type VDCCs. For this reason, we have used both biochemical and electrophysiological methods to investigate the effects of AM404 on VDCCs of mammalian skeletal muscles.

Measurements of Ca^{2+} fluxes through transverse (T)-tubule membranes of skeletal muscle have been used to investigate the functional properties of L-type VDCCs in earlier studies (Dunn, 1989; Oz et al., 2000). T-tubule membranes form sealed inside-out vesicles that are devoid of intracellular organelles (Dunn, 1989). Thus the studies of Ca^{2+} fluxes through these vesicles can be used to measure the activity of VDCCs in their native membranes in the absence of intracellular events such as Ca^{2+} release.

In addition to biochemical methods, electrophysiological techniques have also been employed to investigate the effects of drugs on the function of L-type VDCCs in murine skeletal muscle cells (Cognard et al., 1986; 1993; Neville et al., 1997; Renganathan et al., 1999). In rat myotubes, especially during early periods (1–3 days) in culture medium, majority of calcium currents have been shown to be carried through L-type VDCCs (Cognard et al., 1993). Therefore, we investigated the effects of AM404 on calcium currents mediated by L-type VDCCs in rat

* Corresponding author. National Institute on Drug Abuse / IRP, Integrative Neuroscience Section, 333 Cassell Drive, Baltimore, MD, 21224, USA. Tel.: +1 410 550 1870; fax: +1 410 550 1621.
E-mail address: moz@intra.nida.nih.gov (M. Oz).

0014-2999/$ – see front matter. Published by Elsevier B.V.
doi:10.1016/j.ejphar.2010.02.013

myotubes and on the binding characteristics of [^{3}H]Isradipine, and the function of L-type VDCCs in inside-out T-tubule vesicles isolated from rabbit skeletal muscle.

2. Material and methods

2.1. Preparation of transverse tubule membranes

Microsomal membranes were prepared from the back and hind muscles of small (1–1.5 kg) New Zealand White rabbits, and T-tubules were isolated by sucrose gradient centrifugation as previously described (Dunn, 1989; Oz et al., 2000). The animals were cared for in accordance with the guidelines of the "Guide for the Care and Use of Laboratory Animals" (National Institutes of Health Publication No. 86-23, revised 1985). T-tubule membranes were resuspended and equilibrated in low potassium buffer (10 mM HEPES–Tris, pH: 7.4, 145 mM choline chloride, 5 mM potassium gluconate, 0.02% NaN_3), and stored at −85 °C (Dunn, 1989).

2.2. $^{45}Ca^{2+}$ efflux assay

Approximately 0.4 mg/ml of membranes were loaded with $^{45}Ca^{2+}$ by the addition of one-half volume of isotopically diluted $^{45}CaCl2$ solution in the same buffer to give a final concentration of 5 mM total Ca^{2+} containing approximately 48 μCi/ml $^{45}Ca^{2+}$ (ICN, Irvine, CA, USA). After two freeze-thaw cycles to load the $^{45}Ca^{2+}$, a two-step filtration assay (Dunn, 1989) was used to investigate voltage-dependent $^{45}Ca^{2+}$ efflux. Briefly, 25 μl of loaded membranes were first diluted with 975 μl of high K^+ buffer (10 mM HEPES–Tris, pH 7.4, 120 mM potassium gluconate, 30 mM choline chloride, 0.133 mM EGTA) containing 0.1 μM valinomycin and where appropriate, the test compound. This first dilution is designed to mimic the resting state of the cell by generating an outside negative membrane potential of −80 mV and to reduce the extravesicular (corresponding to intracellular in an inside out vesicle) free Ca^{2+} to less than 100 nM. After 10-min incubation at room temperature, 0.9 ml was removed and applied to a GF/C filter. Excess buffer was removed and 1 ml of depolarizing buffer (10 mM HEPES–Tris pH 7.4, 5 mM potassium gluconate, 145 mM choline chloride, 0.133 mM EGTA, 0.1 mM valinomycin) was added. This two step procedure (F) is referred to as 5–120–5 mM K^+ in the text. Control experiments were carried out using dilution buffers with constant K^+ concentration (5–5–5 mM K+). Efflux was allowed to continue for 15 s and extravesicular solution was removed by rapid washing with a "stop" solution (10 mM HEPES–Tris pH 7.4, 145 mM choline chloride, 5 mM potassium gluconate, 0.5 mM $LaCl_3$, 30 mM sucrose). Filters with their absorbed membrane vesicles were dried, extracted with 5 ml of Hydroflour™ (National Diagnostics, FL, USA) scintillation fluid and counted for $^{45}Ca^{2+}$.

AM404 (N-arachidonoyl-(4-hydroxyphenyl)-amide), VDM11 (N-arachidonoyl-(2-methyl-4- hydroxyphenyl) amine), arachidonylethanolamide, and arachidonic acid were purchased from Tocris (Ellisville, MO, USA). These compounds were dissolved in DMSO. Stocks (100 mM) kept at −20 °C until their use.

2.3. Binding studies

Experiments on the binding of [^{3}H]Isradipine (Specific activity 63.7 Ci/mmol, New England Nuclear, Chadds Ford, PA, USA) were conducted similar to our earlier studies in these membranes (Dunn, 1989). Briefly, aliquots of membranes (0.1 mg) were added to different concentrations of radiolabeled ligand to give a final concentration of 0.02 mg/ml T-tubule membranes in a total volume of 0.8 ml. After 60 min incubation at room temperature, 0.4 ml aliquots of each sample were filtered under vacuum through Watman GF\C filters and rapidly washed with 5 ml of ice-cold assay buffer. The filters were dried and extracted in 5 ml of Hydroflour™ (National Diagnostics, FL, USA). scintillation fluid before counting for ^{3}H. Triplicate 50-μl samples of the incubation mixtures were also counted directly for estimations of total binding. Nonspecific binding was estimated from parallel measurements of binding in the presence of 5 μM unlabeled nifedipine.

2.4. Data analysis

In each experiment, at least 5 determinations were made of the amount of $^{45}Ca^{2+}$ retained by the vesicles under control conditions, i.e. in the absence of any changes in membrane potential and in the absence of drugs. The mean counts per minute (cpm) was first calculated from control determinations and then normalized to 100%. The cpm of each determination was also normalized to the mean cpm to calculate the SEM for each control. Data obtained under other control conditions are expressed as a percentage of control values. Statistical evaluation of data was made using analysis of variance (ANOVA) method. For data analysis and calculations, computer-fitting software Origin™ (Microcal Software, MA, USA) was used.

2.5. Primary cultures of rat skeletal muscle cells

Sprague-Dawley rats (days 1 and 2) were decapitated and hind limb muscles were dissected. Cell dissociation and culture followed described procedures (Neville et al., 1997) with some modifications. Briefly, hind limb muscles from 1–3 pups were dissected in sterile cold Hanks balanced salt (Ca^{2+} and Mg^{2+} free) solution (HBSS: 137 mM NaCl; 5.4 mM KCl; 0.25 mM Na_2HPO_4; 0.44 mM KH_2PO_4; 4.2 mM $NaHCO_3$). Minced tissue was incubated in HBSS containing 0.25% trypsin (w/v) at 37 °C for 20 min and then triturated with Pasteur pipettes of different tip sizes. Visible tissue debris was separated from dispersed cells using a nylon-mesh cell strainer (Invitrogen, Carlsbad, CA). The collected flow-through was centrifuged (10 min. 0–4 °C, 1400 rpm) and the pellet resuspended in Dulbecco's modified Eagle's medium (DMEM) containing 10% fetal calf serum, 200 mM glutamine, 12.5 U/ml penicillin-streptomycin (plating medium). Cells were plated in 35 mm plastic dishes on glass cover-slips coated with 1% gelatin and incubated (in 5% CO_2, water-saturated air) at 37 °C. After 3 days, cells were transferred to differentiation medium (DMEM plus 5% inactivated horse serum). Three days after cell plating colchicine (Sigma; 30 nM) was added to the culture medium to induce formation of rounded myotubes (myoballs) when well-developed myotubes began to appear. All culture media contained penicillin-G (100 U/ml, Sigma) and streptomycin (50 mg/ml, Sigma). Cells were used within two days after the addition of colchicine, since L-type VDCCs constitute the majority of the calcium channel subtype during this period (Cognard et al., 1993).

2.6. Electrophysiological recordings

Cells were voltage-clamped in the whole-cell configuration of the patch-clamp using an Axopatch200B amplifier (Axon Instruments-Molecular Devices, Sunnyvale, CA). Micropipettes were pulled from borosilicate glass to obtain electrode resistances of 3–5 MΩ. The composition of the internal solution (pipette) was (mM): 140 Cs-aspartate; 5 Mg-aspartate, 10 Cs_2EGTA, 10 N-(2-hydroxyethyl) piperazine-N′-(2-ethanesulfonic acid (HEPES), pH was adjusted to 7.4 with CsOH. The external solution used for Ca^{2+} current recording contained (mM): 145 TEA (tetraethylammonium hydroxide)-Br, 10 $CaCl_2$, 10 HEPES and 0.001 tetrodotoxin. Solution pH was adjusted to 7.4 with CsOH. Whole-cell currents were acquired and filtered at 5 kHz with pClamp 6.04 software (Axon Instruments). An interface (Digidata 1200, Axon Instruments) was used for analog-to-digital conversion. For data analysis, integration, and kinetic analysis of current traces computer-fitting software Origin™ version 7.1 (Microcal Software, MA, USA) was used.

3. Results

3.1. The effect of AM404 on voltage dependent $^{45}Ca^{2+}$ fluxes

In the absence of changes in membrane potential (5–5–5 mM K^+ control conditions, C), there was no efflux of $^{45}Ca^{2+}$ from the T-tubule vesicles (Fig. 1A). After repolarization by addition of high external K^+, subsequent depolarization for 15 s (5–120–5 mM K^+ flux conditions; F), the $^{45}Ca^{2+}$ content of the vesicles was reduced to approximately 30–40% of control values. The effects of 15 min incubation with AM404 on $^{45}Ca^{2+}$ effluxes were investigated over a concentration range of 1 to 30 μM. At the highest concentration used (30 μM), AM404 had no appreciable effect on the $^{45}Ca^{2+}$ content of the vesicles under control conditions (Fig. 1A). At a concentration of 3 μM and higher, AM404 significantly decreased the depolarization-dependent $^{45}Ca^{2+}$ effluxes. For example, in the presence of 3 μM AM404, the amount of $^{45}Ca^{+2}$ retained after depolarization of the vesicles was increased from 35 ± 6% to 52 ± 7 % of controls. The difference between these values was statistically highly significant ($P<0.05$, ANOVA, $n=5$–7).

In earlier studies in T-tubule membranes, inhibition of $^{45}Ca^{2+}$ fluxes by endocannabinoids such as AEA and fatty acids such as arachidonic acid was reported (Oz et al., 2000; 2004). Thus the effects of AEA (Fig. 1B) and arachidonic acid (Fig. 1C) were also tested in the presence of 3 μM AM404, to investigate whether AM404 interact with the actions of these compounds on $^{45}Ca^{2+}$ effluxes. Compared to AEA alone, the amount of $^{45}Ca^{+2}$ retained in the vesicles increased significantly in the presence of AM404 and AEA (53 ± 6 % to 69 ± 7 % of controls, respectively; $P<0.05$, ANOVA, $n=6$–7, Fig. 1B). Similarly, compared to arachidonic acid alone, the amount of $^{45}Ca^{+2}$ retained in the vesicles increased significantly in the presence of AM404 and AA (51 ± 5 % to 69 ± 6 % of controls, respectively; $P<0.05$, ANOVA, $n=8$–9, Fig. 1C).

The effect of AM404 was also tested in the presence of VDM11, another AEA transport inhibitor (De Petrocellis et al., 2000), to determine whether AM404 continues to inhibit on $^{45}Ca^{2+}$ effluxes after the inhibition of AEA transport process After 15 min coincubation of membranes in 1 μM VDM11 and 3 μM AM404 the amount of $^{45}Ca^{+2}$ retained in the T-tubule vesicles increased significantly in the presence of AM404 ($P<0.05$, ANOVA, $n=7$–8, Fig. 1D). VDM11 alone was tested at two concentrations (1 μM and 10 μM). Although, 1 μM VDM11 did not alter $^{45}Ca^{2+}$ effluxes (Fig. 1D), 10 μM VDM11 caused a significant inhibition of $^{45}Ca^{2+}$ effluxes (24 ± 5% increase in $^{45}Ca^{+2}$ retained in the vesicles; $P<0.05$, ANOVA, $n=7$–9) indicating that VDM11, albeit with lower potency, also interacts with VDCCs.

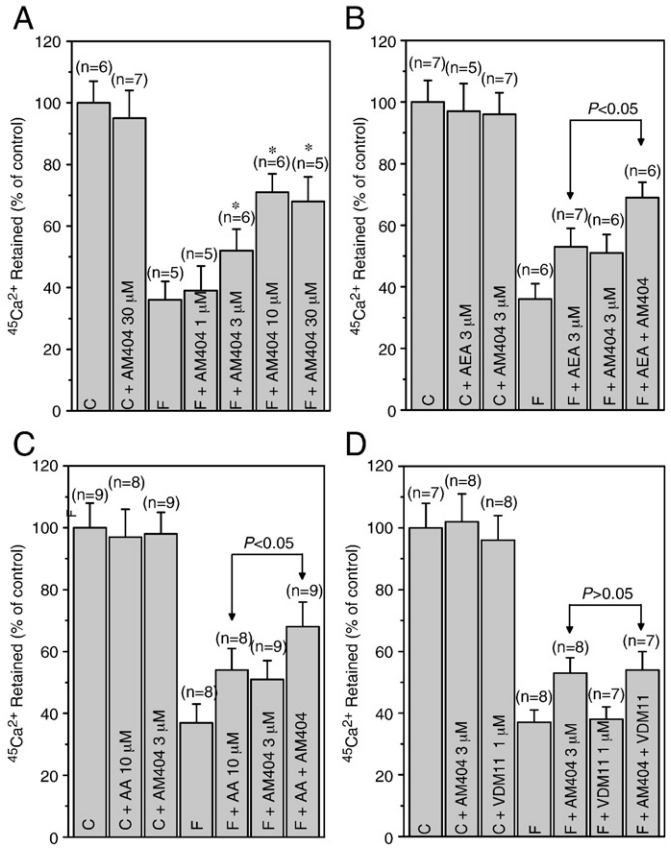

Fig. 1. Effects of AM404 on $^{45}Ca^{2+}$ fluxes through T-tubule membranes. A) Effects of increasing concentrations of AM404 on depolarization-induced $^{45}Ca^{2+}$ effluxes. B) Effects of AM404 on AEA-induced inhibition of depolarization-induced $^{45}Ca^{2+}$ effluxes. C) Effects of AM404 on AA-induced inhibition of depolarization-induced $^{45}Ca^{2+}$ effluxes. D) Effects of AEA transport inhibitor VDM11 on AM404-induced inhibition of depolarization-induced $^{45}Ca^{2+}$ effluxes. The numbers of experiments (n) and the values of S.E.M. are indicated on top of each column. Statistical significance at the level of $P<0.05$ was presented with *. C, control conditions; F, flux conditions. AEA, anandamide; AA, arachidonic acid.

3.2. The effects of AM404 on the binding of [^{3}H]Isradipine

In radioligand binding experiments, the effect of 10 μM AM404 was investigated on the specific binding of DHP-class ligand [^{3}H]Isradipine. Equilibrium curves for the binding of [^{3}H]Isradipine, in the presence and absence of the AM404 are presented in Fig. 2A ($n=4$–5). At a concentration of 10 μM, AM404 caused a significant inhibition of the specific binding of [^{3}H]Isradipine. Maximum binding activities (B_{max}) of [^{3}H] Isradipine were 51.4 ± 6.1 and 27.3 ± 5.2 pM/mg (means ± SEM) for controls and AM404, respectively (Fig. 2A). The apparent affinity (KD) of the receptor for [^{3}H]Isradipine was 236 ± 43 and 220 ± 37 pM for controls and AM404, respectively. There were no statistically significant difference between control and AM404 treated groups with respect to both KD and the B_{max} values ($P>0.05$, ANOVA, $n=5$–6). The effect of AM404 were also investigated on the displacement of specific [^{3}H] Isradipine binding from T-tubule membranes (Fig. 2B). In the concentration range used (0.1 to 30 μM), AM404 caused a significant inhibition of the specific binding of [^{3}H]Isradipine. The values for IC_{50} and slope factor for the AM404 were 4.7 μM and 1.5, respectively.

The effects of AEA and arachidonic acid on the specific [^{3}H]Isradipine binding from T-tubule membranes, were also investigated in the absence (controls) and presence of AM404 (Fig. 2C; $n=4$–5). Compared to controls, inhibitory effect of AEA (3 μM) and arachidonic acids (10 μM) on the specific binding of [^{3}H]Isradipine was enhanced significantly in the presence of 3 μM AM404 (Fig. 2C). Finally, the effect of AM404 on the specific binding of [^{3}H]Isradipine was tested in the presence of VDM11 (1 μM) Maximum binding activities (B_{max}) of [^{3}H] Isradipine for controls ($n=6$), AM404 ($n=6$), VDM11 ($n=8$), and AM404 + VDM11 ($n=8$) treatment groups were 41.2 + 5.1, 38.7 ± 6.3, 21.6 ± 3.7, and 19.8 ± 4.1 pM/mg, respectively (Fig. 2D). The apparent affinities (KD) of the receptor for [^{3}H]Isradipine were 239 ± 53, 236 ± 47, 223 ± 58 and 220 ± 41 pM for controls, AM404, VDM11 and AM404 + VDM11, respectively.

3.3. The effects of AM404 on the L-type calcium currents recorded in rat skeletal muscle myotubes

Rat myotubes has been routinely used to study functional and pharmacological characteristics of L-type VDCCs of mammalian skeletal muscles (Cognard et al., 1986, 1993; Neville et al., 1997; Renganathan et al., 1999). Using whole cell configuration of patch-clamp technique, we investigated the effects of AM404 on Ca^{2+} currents mediated by L-type VDCCs in rat myotubes. In agreement with earlier studies, in voltage-clamp mode, depolarizing test pulses (0.5 s applied every 30 s) from holding potential of −80 mV to +10 mV induced slowly activating L-type VDCCs which was blocked by 1 μM Isradipine (data

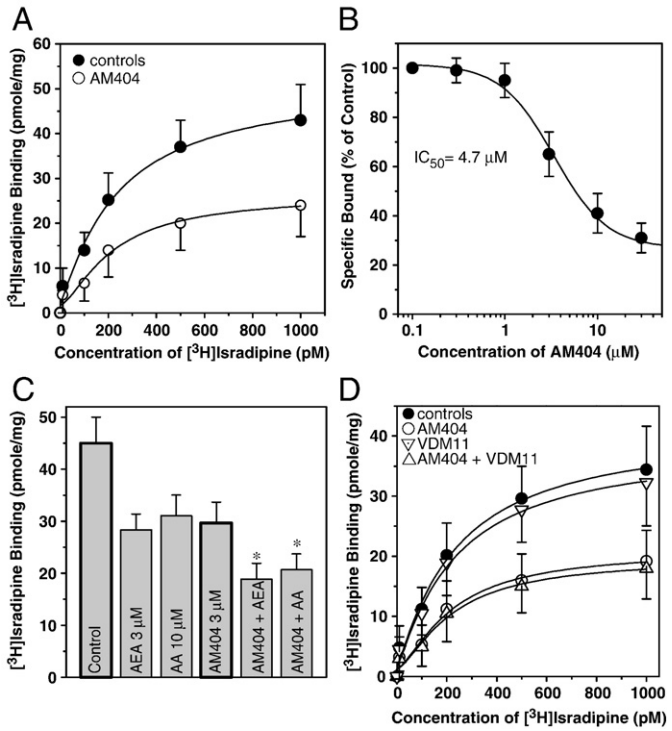

Fig. 2. The effects of AM404 on the specific binding of [^{3}H]Isradipine to T-tubule membranes. A) In the presence and absence of AM404, specific binding as a function of the concentration of [^{3}H]Isradipine. Data points for controls and AM404 (10 μM) are indicated by (●) and (○), respectively. B) The effects of increasing concentrations of AM404 on the specific binding of [^{3}H]Isradipine to T-tubule membranes The IC_{50} values for the compounds used were obtained from nonlinear regression fits of the data points. Membranes were incubated with 0.5 nM [^{3}H]Isradipine at a concentration of 0.02 mg/ml for 1 h with increasing concentrations of compounds in the medium. Bound and free [^{3}H]Isradipine were separated by filtration. C) The effects of co-application of AM404 (3 μM) with AEA (3 μM) or AA (10 μM) on the specific binding of [^{3}H]Isradipine to T-tubule membranes. Data are expressed as percentage of control. Symbols are the means of 5–6 experiments. Vertical lines on data points represent the S.E.M. Statistical significance compared to AM404 alone at the level of $P<0.05$ was presented with *. D) In the presence and absence of VDM11, specific binding as a function of the concentration of [^{3}H]Isradipine. Data points for controls, VDM11 (1 μM), AM404 (10 μM), and AM404 + VDM11 are indicated by ●, ▽, ○, and △, respectively. Data are presented as the arithmetic means of 4–5 experimental measurements. Solid lines were calculated from the best-fit parameters obtained by nonlinear curve fitting to a single-site binding equation.

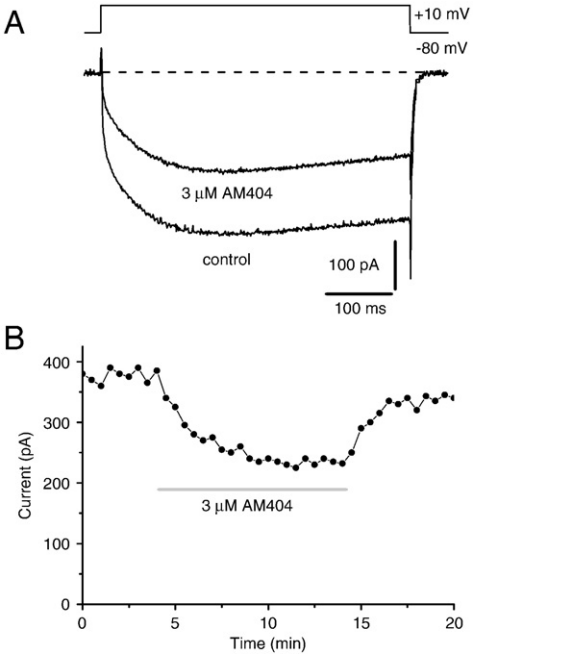

Fig. 3. The effect of AM404 on Ca^{2+} currents mediated by L-type voltage-dependent calcium channels in rat myotubes. A) AM404 inhibits calcium currents recorded using whole-cell voltage-clamp mode of patch clamp technique. Current traces recorded before (control) and 10 min after 3 μM AM404 application were presented. Depolarizing test pulses to +10 mV for 0.5 s was elicited from holding potential of −80 mV at every 30 s. B) Time course of AM404 inhibition of L-type voltage-dependent calcium channels. Following a 4 min baseline recording, AM404 (3 μM) was included in extracellular solution for 10 min (horizontal bar).

not shown, $n=3$). Extracellular application of 3 μM AM404 for 10 min caused a significant inhibition of Ca^{2+} currents mediated through L-type VDCCs (Fig. 3A). The inhibitory effect of AM404 developed gradually with in 10 min and recovered partially after the cessation of AM404 application (Fig. 3B). The average maximal current amplitudes before and 10 min after 3 μM AM404 application were 340 ± 23 nA in controls and 203 ± 25 nA in AM404 (mean ± SEM; $n=5$, $P<0.05$, paired t-test), respectively. The studying the effect of increasing AM404 concentrations, indicated that AM404 inhibits the maximal amplitudes of VDCC with an IC_{50} value of 3.2 μM ($n=4$–5; Fig. 4A). Maximal inhibition of approximately 60% inhibition was obtained in the concentration range of 10 to 30 μM AM404. Current–voltage relationship of Ca^{2+} currents recorded in the absence and presence of 3 μM AM404 ($n=5$) indicated that the inhibitory effect of AM404 is not dependent on the membrane potential (Fig. 4B).

Time to peak currents (142 ± 34 ms for controls versus 154 ± 29 ms in AM404; paired t-test, $P>0.05$) was not altered significantly in the presence of 3 μM AM404 (Fig. 4C). Similarly, there were no statistically significant differences between the means of inactivation time constants before (control) and after AM404 application (584 ± 49 ms for controls versus 611 ± 53 ms in AM404; paired t-test, $P>0.05$). In another set of experiments, we have increased the frequency of pulse stimulations to test whether increasing the time channels stay open affects AM404 inhibition of L-type VDCCs. The extent of AM404 inhibition of L-type VDCCs stimulated every 30, 60, and 120 s were presented in Fig. 4D. Increasing the concentration of stimulation frequencies did not alter the extent of AM404 inhibition of L-type VDCCs, suggesting that the changes in the opening frequency of VDCC do not alter the inhibitory effect of AM404.

4. Discussion

The results indicate that AM404 inhibits both the function of L-type VDCCs and the binding of [^{3}H]Isradipine in T-tubule membranes of rabbit skeletal muscle. In agreement with these findings, AM404 inhibited currents mediated by L-type VDCCs in cultured rat skeletal muscle cells. This is, to our knowledge, the first study reporting a direct effect of AM404, an AEA transport inhibitor on the function of L-type VDCCs.

In earlier investigations, a high density of specific DHP binding sites (Dunn, 1989) and the presence of functional Ca^{2+} channels corresponding to these binding sites have been demonstrated in T-tubule membranes of skeletal muscle (Flockerzi et al., 1986). The depolarization-induced $^{45}Ca^{2+}$ fluxes through T-tubule vesicles used in this study have been shown to be blocked by established inorganic and organic blockers of L-type channels (Dunn, 1989; Oz et al., 1993). Thus, in the present study, the effects of AM404 on both radioligand binding and the functional aspect of the VDCCs have been studied in a pharmacologically well-characterized assay system. Furthermore, since the function of VDCCs are regulated significantly by the changes in intracellular Ca^{2+} and/or second messenger systems including protein kinases C, A, and calmodulin (Soldatov et al., 1998; Oz et al., 1998), it is possible that the reported effects of AM404 on these second messenger systems contribute to its actions on VDCCs (Chen et al., 2001; Jonsson et al., 2003; De Lago et al., 2006; Chang et al., 2008). However, it is unlikely that the observed effects of AM404 on $^{45}Ca^{2+}$ fluxes through

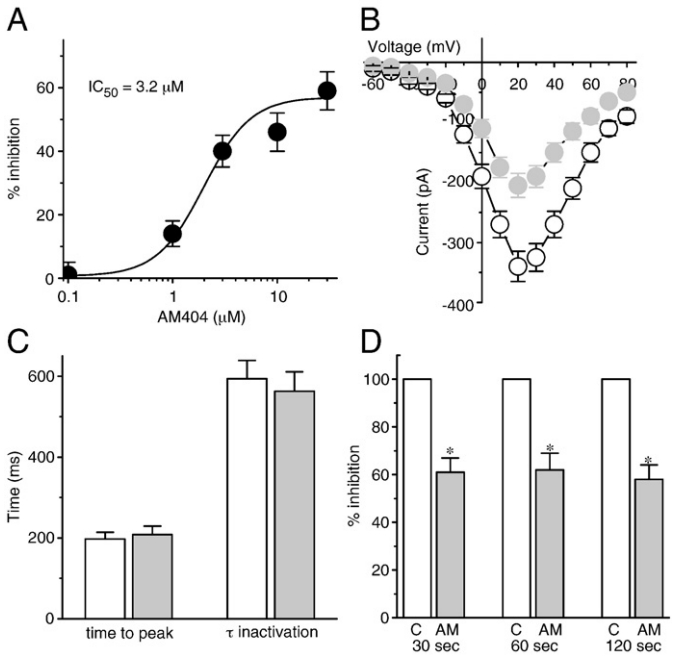

Fig. 4. The effect of AM404 on the maximal current amplitudes, kinetics of calcium currents, and the currents stimulated at different pulse frequencies. A) The effects of increasing concentrations of AM404 on the maximal current amplitudes. The IC_{50} value was obtained from nonlinear regression fits of the data points ($n=4$–5 cells). B) Current–voltage relationship of Ca^{2+} currents recorded in the absence (black filled circles) and presence (gray filled circles) of 3 μM AM404. Currents were evoked by the 500 ms depolarizing voltage steps from holding potential of −80 mV to command potentials ranging from −60 to +80 mV. Data points present the mean and S.E.M. values from 5 cells. C) The effect of AM404 on the kinetics of L-type VDCCs. Means and the S.E.M. of the time to reach peak amplitude and inactivation time constant (τ) were presented before (control, white bars) and 10 min after (grey bars) 3 μM AM404 application ($n=5$ cells). D) The extent of AM404 inhibition of L-type VDCCs at varying pulse intervals. The extent of inhibition was calculated from the maximal current amplitudes before (controls, white bars) and after AM404 (grey bars) application at the stimulation intervals indicated in the figure. Control and treatment groups were calculated and normalized separately for each stimulation interval group ($n=4$–5 cells). The S.E.M. values are indicated on top of each column. * Indicates statistical significance at the level of $P<0.05$ (paired t-test). C, control conditions; AM, AM404.

these vesicles involve changes in intracellular Ca^{2+}, since the T-tubule vesicles are in an inside-out orientation and devoid of intracellular organelles (Dunn, 1989).

In agreement with our studies in rabbit T-tubule membranes, AM404 also inhibited L-type of VDCCs in cultured rat skeletal muscle cells. The effect of AM404 on Ca^{2+} currents developed gradually reached a plateau with in 10 min and recovered partially during washout period. The relatively slow time course for the effect and the recovery periods of AM404 is likely due to the lipophilic nature of this compound. Time to reach peak current amplitude and the inactivation kinetics were not altered in the presence of AM404. Current–voltage relationship indicated that the AM404 inhibition was not dependent on the membrane potential. Further studies using different stimulation frequencies suggested that AM404 induced inhibition is independent of the channel openings, and AM404 interact with the closed state of the channel. Similar findings indicating the fatty acids and fatty acid-based compounds interact with the closed state of L-type VDCCs have been reported in several earlier studies (for recent reviews Oz, 2006; Boland and Drzewiecki, 2008; Roberts-Crowley et al., 2009).

AM404, in the low μM concentration range used in this study, has been shown to bind cannabinoid receptors (Khanolkar, et al., 1996; Zygmunt et al., 2000). Since, the inhibition of $^{5}Ca^{2+}$ fluxes by AEA was not inhibited by SR141716A, CB1 receptor antagonist and WIN55212-2, synthetic cannabinoid receptor agonist, did not mimic the actions of AEA in T-tubule membranes (Oz et al., 2000, 2004), it is not likely that the activation of cannabinoid receptors mediate the effects of AM404 on $^{5}Ca^{2+}$ fluxes. In earlier studies, both the expression of vanilloid receptors in the skeletal muscle tissue (Cavuoto et al., 2007), and the activation of these receptors by AM404 have been demonstrated (Zygmunt et al., 2000). However, the vanilloid receptor antagonist, capsazepine (1 μM) did not reverse the inhibitory effect of AM404 on $^{45}Ca^{2+}$ fluxes (unpublished results, $P>0.05$, ANOVA, $n=5$–7). Furthermore, in the present and earlier studies (Oz et al., 2000, 2004), AEA, in concentrations shown to activate vanilloid receptors did not cause alterations in the amount of $^{45}Ca^{2+}$ retained in the membrane vesicles under control conditions, suggesting that vanilloid receptors are not involved in observed effects of AM404 in T-tubule membranes.

The additive effects of AM404 and AEA observed in this study could be due to inhibition of AEA transport process. However, the AM404 continued to inhibit $^{45}Ca^{2+}$ fluxes and specific DHP binding in the presence of VDM11, another AEA transport inhibitor. Thus, the inhibition of AEA transport process may not be involved in observed effects of AM404. In addition, AM404 potentiated the effects of not only AEA but also arachidonic acid, suggesting that its interaction with AEA on $^{45}Ca^{2+}$ fluxes is not specific. Furthermore, due to the inside-out orientation of T-tubule membranes, AM404 alone or in combination with AEA does not need to be transported to the cytoplasmic compartment. In agreement with our findings, AM404 has been shown to modulate directly the functions of voltage-gated sodium channels (Nicholson et al., 2003; Kelley and Thayer, 2004) and T-type Ca^{2+} channels (Chemin et al., 2001). Interestingly, 10 μM AM404 perse caused approximately 30% inhibition of T-type Ca^{2+} channels and the effects of AEA was blocked in the presence of AM404, suggesting that AM404 and AEA shares similar sites for their actions on these channels (Chemin et al., 2001).

Several cellular events such as intracellular Ca^{2+} release (Chen et al., 2001; Chang et al., 2008), cellular toxicity (De Lago et al., 2006), proliferation (Jonsson et al., 2003), and the nuclear regulatory processes by transcription factors (Caballero et al., 2007) are also modulated directly by AM404. Importantly, in some of the recent studies, it has been reported that the AM404-induced behavioral changes are not attributable to inhibition of AEA transport mechanism (Cippitelli et al., 2007; Trezza and Vanderschuren, 2009).

Results of the present study indicate that AM404, in the concentrations of 3 μM and higher, causes a significant suppression of $^{45}Ca^{2+}$ fluxes mediated by VDCCs in T-tubules of skeletal muscle. In addition these data indicate that AM404 and AEA have additive inhibitory effects on the [^{3}H]Isradipine binding and high-K-induced $^{45}Ca^{2+}$ fluxes. However, the potentiation of AEA actions by AM404 does not appear to be due to the inhibition of AEA transporter. In conclusion, the results suggest that AM404 modulates the function of L-type VDCCs and inhibits the binding of [^{3}H]Isradipine in mammalian muscle cells and membranes in a manner independent of AM404 actions on the AEA transport process.

Acknowledgments

This study was in part supported by the Intramural Research Program of the NIDA/NIH, USA and the United Arab Emirates University Research Funds.

References

Boland, L.M., Drzewiecki, M.M., 2008. Polyunsaturated fatty acid modulation of voltage-gated ion channels. Cell Biochem. Biophys. 52, 59–84.

Caballero, F.J., Navarrete, C.M., Hess, S., Fiebich, B.L., Appendino, G., Macho, A., Muñoz, E., Sancho, R., 2007. The acetaminophen-derived bioactive N-acylphenolamine AM404 inhibits NFAT by targeting nuclear regulatory events. Biochem. Pharmacol. 73, 1013–1023.

Cavuoto, P., McAinch, A.J., Hatzinikolas, G., Janovská, A., Game, P., Wittert, G.A., 2007. The expression of receptors for endocannabinoids in human and rodent skeletal muscle. Biochem. Biophys. Res. Commun. 364, 105–110.

Chang, H.T., Huang, C.C., Cheng, H.H., Wang, J.L., Lin, K.L., Hsu, P.T., Tsai, J.Y., Liao, W.C., Lu, Y.C., Huang, J.K., Jan, C.R., 2008. Mechanisms of AM404-induced [Ca(2+)](i) rise and death in human osteosarcoma cells. Toxicol. Lett. 179, 53–58.

Chemin, J., Monteil, A., Perez-Reyes, E., Nargeot, J., Lory, P., 2001. Direct inhibition of T-type calcium channels by the endogenous cannabinoid anandamide. EMBO J. 20, 7033–7040.

Chen, W.C., Huang, J.K., Cheng, J.S., Tsai, J.C., Chiang, A.J., Chou, K.J., Liu, C.P., Jan, C.R., 2001. AM-404 elevates renal intracellular Ca(2+), questioning its selectivity as a pharmacological tool for investigating the anandamide transporter. J. Pharmacol. Toxicol. Methods 45, 195–198.

Cippitelli, A., Bilbao, A., Gorriti, M.A., Navarro, M., Massi, M., Piomelli, D., Ciccocioppo, R., Rodríguez de Fonseca, F., 2007. The anandamide transport inhibitor AM404 reduces ethanol self-administration. Eur. J. NeuroSci. 26, 476–486.

Cognard, C., Romey, G., Galizzi, J.P., Fosset, M., Lazdunski, M., 1986. Dihydropyridine-sensitive Ca^{2+} channels in mammalian skeletal muscle cells in culture: electrophysiological properties and interactions with Ca^{2+} channel activator (Bay K8644) and inhibitor (PN 200-110). Proc. Natl. Acad. Sci. U. S. A. 83, 1518–15122.

Cognard, C., Constantin, B., Rivet-Bastide, M., Imbert, N., Besse, C., Raymond, G., 1993. Appearance and evolution of calcium currents and contraction during the early post-fusional stages of rat skeletal muscle cells developing in primary culture. Development 117, 1153–1161.

De Lago, E., Gustafsson, S.B., Fernández-Ruiz, J., Nilsson, J., Jacobsson, S.O., Fowler, C.J., 2006. Acyl-based anandamide uptake inhibitors cause rapid toxicity to C6 glioma cells at pharmacologically relevant concentrations. J. Neurochem. 99, 677–688.

De Petrocellis, L., Bisogno, T., Davis, J.B., Pertwee, R.G., Di Marzo, V., 2000. Overlap between the ligand recognition properties of the anandamide transporter and the VR1 vanilloid receptor: inhibitors of anandamide uptake with negligible capsaicin-like activity. FEBS Lett. 483, 52–56.

Di Marzo, V., 2008. Endocannabinoids: synthesis and degradation. Rev. Physiol. Biochem. Pharmacol. 160, 1–24.

Dunn, S.M.J., 1989. Voltage-dependent calcium channels in skeletal muscle transverse tubules: measurements of calcium efflux in membrane vesicles. J. Biol. Chem. 264, 11053–11060.

Flockerzi, V., Oeken, H.J., Hofmann, F., Pelzer, D., Cavalie, A., Trautwein, W., 1986. Purified dihydropyridine-binding site from skeletal muscle T-tubules is a functional channel. Nature 323, 66–68.

Fowler, C.J., 2008. "The tools of the trade" — an overview of the pharmacology of the endocannabinoid system. Curr. Pharm. Des. 14, 2254–2265.

Howlett, A.C., Barth, F., Bonner, T.I., Cabral, G., Casellas, P., Devane, W.A., Felder, C.C., Herkenham, M., Mackie, K., Martin, B.R., Mechoulam, R., Pertwee, R.G., 2002. International Union of Pharmacology. XXVII. Classification of cannabinoid receptors. Pharmacol. Rev. 54, 161–202.

Jonsson, K.O., Andersson, A., Jacobsson, S.O., Vandevoorde, S., Lambert, D.M., Fowler, C.J., 2003. AM404 and VDM 11 non-specifically inhibit C6 glioma cell proliferation at concentrations used to block the cellular accumulation of the endocannabinoid anandamide. Arch. Toxicol. 77, 201–207.

Kelley, B.G., Thayer, S.A., 2004. Anandamide transport inhibitor AM404 and structurally related compounds inhibit synaptic transmission between rat hippocampal neurons in culture independent of cannabinoid CB1 receptors. Eur. J. Pharmacol. 496, 33–39.

Khanolkar, A.D., Abadji, V., Lin, S., Hill, W.A.G., Taha, G., Abouzid, K., Meng, Z., Fan, P., Makriyannis, A., 1996. Head group analogs of arachidonylethanolamide, the endogenous cannabinoid ligand. J. Med. Chem 39, 4515–4519.

Neville, C., Rosenthal, N., McGrew, M., Bogdanova, N., Hauschka, S., 1997. Skeletal muscle cultures. In: Emerson, C.P., Sweeney, H.L. (Eds.), Methods in muscle biology. Academic Press, San Diego, pp. 85–116.

Nicholson, R.A., Liao, C., Zheng, J., David, L.S., Coyne, L., Errington, A.C., Singh, G., Lees, G., 2003. Sodium channel inhibition by anandamide and synthetic cannabimimetics in brain. Brain Res. 978, 194–204.

Oz, M., 2006. Receptor-independent effects of endocannabinoids on ion channels. Curr. Pharm. Des 12, 227–239.

Oz, M., Frank, G.B., Dunn, S.M.J., 1993. Voltage-Dependent Calcium Flux Across Rabbit Skeletal Muscle Transverse Tubule Membranes in the Range of Late After Potentials. Can. J. Pharmacol. Physiol. 71, 518–521.

Oz, M., Melia, M.T., Soldatov, N., Abernethy, D.R., Morad, M., 1998. Functional coupling of human L-type Ca^{2+} channel and angiotensin AT1A receptor co-expressed in Xenopus oocytes: Involvement of the carboxyl-terminal Ca^{2+} sensors. Mol. Pharmacol. 54, 1106–1112.

Oz, M., Tchugunova, Y., Dunn, S.M.J., 2000. Endogenous cannabinoid anandamide directly inhibits voltage-dependent calcium fluxes in rabbit T-tubule membrane preparations. Eur. J. Pharmacol. 404, 13–20.

Oz, M., Tchugunova, Y., Dinc, M., 2004. Differential effects of endocannabinoids and synthetic cannabinoids on voltage-dependent calcium fluxes in rabbit t-tubule membranes; comparison with fatty acids. Eur. J. Pharmacol. 502, 47–58.

Oz, M., Alptekin, A., Tchugunova, Y., Dinc, M., 2005. Effects of saturated long-chain N-acylethanolamines voltage-dependent calcium fluxes in rabbit t-tubule membranes. Arch. Biochem. Biophys. 434, 344–351.

Renganathan, M., Wang, Z.M., Messi, M.L., Delbono, O., 1999. Calcium regulates L-type Ca^{2+} channel expression in rat skeletal muscle cells. Pflugers Arch. 438, 649–655.

Roberts-Crowley, M.L., Mitra-Ganguli, T., Liu, L., Rittenhouse, A.R., 2009. Regulation of voltage-gated Ca^{2+} channels by lipids. Cell Calcium 45, 589–601.

Soldatov, N., Oz, M., O'Brien, K.A., Abernethy, D.R., Morad, M., 1998. Molecular determinants of L-type Ca^{2+} channel inactivation. J. Biol. Chem. 273, 957–963.

Trezza, V., Vanderschuren, L.J., 2009. Divergent effects of anandamide transporter inhibitors with different target selectivity on social play behavior in adolescent rats. J. Pharmacol. Exp. Ther. 328, 343–350.

Zygmunt, P.M., Chuang, H., Movahed, P., Julius, D., Högestätt, E.D., 2000. The anandamide transport inhibitor AM404 activates vanilloid receptors. Eur. J. Pharmacol. 396, 39–42.